RIPPLE ORIENTATIONS AS INDICATORS OF RECENT SURFACE WINDS ON MARTIAN SAND DUNES. J. R. Zimbelman[1] and M. B. Johnson[1], [1]Center for Earth and Planetary Studies, National Air and Space Museum, Smithsonian Institution, Independence Ave. & 6th St. SW, Washington, DC 20013: zimbelmanj@si.edu.

Introduction: Sand dunes on both Earth and Mars have been shown to preserve the most recent wind patterns in their ripple formations [1-3]. This investigation, supported by NASA MDAP grant NN12AJ38G [4], summarizes documentation of wind ripples on Martian dunes from across Mars in order to assess recent surface wind flows. This information will provide insight into the modes of dune formation and ripple morphology at the study sites, and offer new constraints for global or regional circulation models.

Background: Movement of Martian sand ripples was first observed by the Spirit rover [5] but ripples now can be studied using images from the High Resolution Imaging Science Experiment (HiRISE) camera [6, 7]. This instrument provides unprecedented views of Mars, including sand dunes in diverse areas, with resolution as high as 25 cm/pixel [6]. This includes dunes with complex structures and crest positions which may have been created by multiple wind directions or seasonal wind variations. Being unable to choose between multiple possible regimes leaves some dune morphologies open to interpretation. However, dune crests and ripples mapped by Neilson and Kocurek [1] show that the ripple patterns are a good indicator of recent surface wind flow which modifies the principle crests. This same ripple mapping technique now can be used to document recent wind flow patterns on Mars. Because wind speeds have yet to be measured directly in most areas, we must rely on high resolution images and ripple-scale patterns for recent wind information.

Methodology: The Martian study sites used in this investigation were selected to have clear HiRISE images of ripples on sand dunes, and be able to represent diverse locations across the surface as determined primarily by their latitude and longitude. Frames with stereo pairs were preferred when available because of the ability to create digital terrain models (DTMs) of the sites using photogrammetry software such as SOCET SET. The resulting 40 study sites and their corresponding HiRISE images are listed in Table 1, and their global distribution illustrated in Figure 1. The ripple documentation method at the first 7 sites used the Java Mission-planning and Analysis for Remote Sensing (JMARS) geospatial information system (GIS) while the remaining images were studied using ESRI's Arc GIS. In both systems, lines were drawn perpendicular to ripple crests across three adjacent ripples in order to document ripple wavelength from line length

Site	Region	HiRISE frame ID	Lon E	Lat
1	Hellespontus	PSP_007663_1350	38.779	-44.859
2	Gale Crater	PSP_009571_1755	137.497	-4.463
3	Nili Patera	ESP_017762_1890	67.321	8.779
4	North Polar	PSP_010019_2635	118.543	83.505
5	Aonia Terra	ESP_013785_1300	293.1	-49.804
6	Lus Chasma	ESP_027341_1720	276.387	-7.718
7	Arabia Terra	ESP_016459_1830	4.553	3.12
8	Terra Cimmeria	ESP_025645_1455	138.437	-34.23
9	Lyot Crater	PSP_009746_2290	29.287	48.864
10	Icaria Planum Crater	ESP_029478_1350	259.932	-44.482
11	South of Promethei Terra	ESP_022731_1080	143.002	-71.68
12	Terra Sirenum	ESP_023928_1205	218.035	-59.098
13	Vastitas Borealis	ESP_018925_2520	344.658	71.906
14	Milankovic Crater	ESP_018930_2350	213.42	54.576
15	Becquerel Crater	PSP_001955_2015	351.899	21.445
16	Terra Tyrrhena	ESP_026675_1655	97.769	-14.552
17	Gamboa Crater	PSP_002721_2210	315.704	40.78
18	Aeolis Mensae	PSP_010178_1825	122.357	2.247
19	Wirtz Crater	ESP_021893_1315	334.676	-48.243
20	Near Cerberus Fossae	PSP_008449_1885	169.194	8.566
21	Coprates Chasma	ESP_026905_1660	296.894	-14.092
22	Kaiser Crater	PSP_007110_1325	18.794	-46.98
23	North Polar	ESP_027474_2610	223.471	80.832
24	Syrtis Major Planum	ESP_019845_2000	79.425	19.823
25	West of Daedalia Planum	ESP_024838_1630	207.988	-16.72
26	Herschel Crater	PSP_006974_1635	128.39	-16.391
27	Capen Crater	ESP_026757_1865	13.958	6.349
28	South of Eos Chasma	ESP_025625_1580	320.382	-21.603
29	Promethei Terra	ESP_023285_1230	133.179	-56.923
30	Terra Sirenum	ESP_023731_1405	195.967	-38.96
31	Arabia Terra	ESP_033454_2065	57.027	26.149
32	North of Kasei Valles	ESP_025177_2145	306.143	34.13
33	Ganges Chasma	PSP_008536_1725	314.784	-7.409
34	Bunge Crater	ESP_018650_1460	311.226	-33.534
35	Crater within Schiaparelli (	PSP_002930_1800	14.404	-0.094
36	Pettit Crater	ESP_037603_1920	185.888	11.804
37	Meridiani Region	ESP_016789_1720	356.118	-7.716
38	Meridiani Terra	ESP_033483_1805	348.773	0.493
39	Huygens Crater	ESP_036131_1675	56.717	-12.274
40	Richardson Crater	ESP_031749_1080	179.402	-72.008

Table 1. Location and HiRISE frame information for the 40 study sites where ripple measurements were documented. Sites are listed in order of completion, and they are spatially widely distributed around Mars (see Fig. 1).

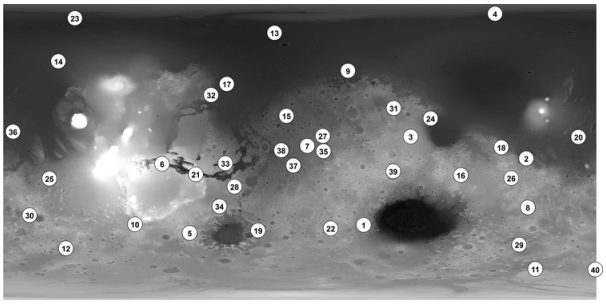

Figure 1. The 40 ripple study site locations (Table 1) represented on a gray-scale MOLA elevation map.

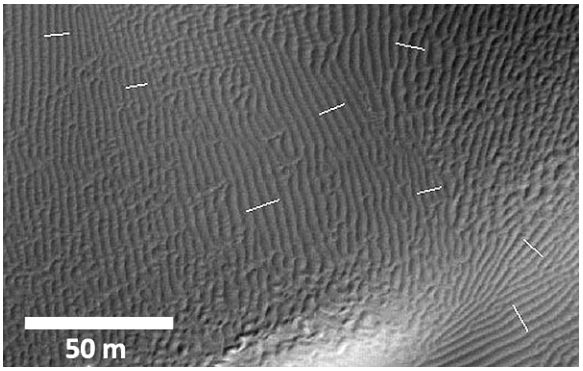

Figure 2. Ripples mapped with lines perpendicular to crests. Regions with complex or overlapping patterns were avoided. Site 8, Terra Cimmeria (Table 1).

and inferred wind direction from azimuth (Fig. 2). It is not possible to infer a unique wind direction from ripple orientation alone and therefore the inferred directions have a 180 degree ambiguity [8]. For example, a crest with North-South alignment may have been constructed by an Easterly, Westerly, or bi-directional wind. Due to this ambiguity, results obtained during this study will assume azimuths to be between 0 and 180 degrees. Actual orientations may be defined after further study by using additional information about dune morphology [3], such as well-known dune types and the rule of maximum gross bedform-normal transport [9]. Ripples in each study site are then categorized by the cardinal wind direction they suggest and percentages of each inferred direction are calculated. Percentages of wavelength values are also displayed in order to look for possible regional or global patterns. At sites with existing DTMs, inferred wind direction can be compared to the slope magnitude on which the ripple formed [10]. The slope information allowed us to evaluate how great the effect of slope may be on deflecting ripple orientation on Martian dunes [10], using the results first described for sand dunes on Earth by Howard [11].

Terra Sirenum Example: One site explored during this study is in Terra Sirenum (HiRISE frame ESP_023928_1205, site 12 in Table 1), where 333 ripples were recorded using lines perpendicular to the ripple crests. In this area, about 1% of measurements suggest an ESE-WNW wind, 36% suggest SE-NW, 38% suggest SSE-NNW, 24% suggest S-N, and the remaining 1% suggest SSW-NNE. This distribution shows that the wind was primarily in a SSE-NNW with additional ripple orientations distributed around this direction. Ripple wavelength ranged from 2 to 4 meters, where 3-4 m represents the majority of measurements in the ESE and SE while 2-3 m comprise the majority of SSE, S, and SSW measurements. It is unclear if any strong relationship exists between ripple orientation and wavelength. The slope distribution on the dunes at this site indicates that very few (<5%) of the ripple measurements were obtained on slopes >15°. However, these few measurements fell into two of the larger orientation categories (SSE-NNW and S-N), so that any possible effect on the overall distribution should be minimized. One small dune at this site examined in detail shows that while the angle between the direction of inferred wind and direction of maximum slope ranges between 13 and 87 degrees, the ripples show a NW-SE wind over the majority of the dune, with only minimal variation at the base of the eastern side where form flow effects may have occurred [8]. These results confirm that slope does not seem to have a large affect on ripple orientation and deflection, as long as areas on or next to slip faces are avoided [10].

Results: The Martian surface displays an abundance of sand dunes in many different areas [e.g., 12], and the ripple patterns visible on some dunes provide a new tool for gaining insight into the most recent sand-moving winds [2, 3]. The complexity of documented ripple patterns varies from uniform directionality across hundreds of kilometers to areas with varying patterns on a single dune, plus overlapping ripple patterns at many locations (but such areas were not included in the present study). These patterns suggest the possiblity of regional variations between single and multiple dominant winds, perhaps including a diurnal or seasonal change in the wind direction. Individual study sites suggest that there may be a relationship between ripple wavelength and azimuth, although more study is needed to evaluate how rigorous any relationship may be. Finally, surface slope angle on the dunes does not have a significant effect on the deflection of ripple orientation with respect to the formational wind as long as areas adjacent to slip faces are avoided.

References: [1] Neilson J. and Kocurek G. (1987) *Geol. Soc. Am. Bull., 99,* 177-186. [2] Ewing R. et al. (2010) *J. Geophys. Res., 115,* E08005. [3] Liu Z. and Zimbelman J. (2015) *Icarus*, 261, 169-181. [4] Zimbelman J. (2011) NSPIRES NNH11ZDA001N-MDAP. [5] Sullivan R. et al. (2008) *J. Geophys. Res., 113,* E06S07. [6] McEwen A. et al. (2007) *J. Geophys. Res., 112*, E05S02. [7] Bridges N. et al. (2012) *Nature, 485,* 339-342. [8] Johnson M. and Zimbelman J. (2015) LPSC 46, Abs. 1539. [9] Fenton L. et al. (2014) *Icarus, 230,* 5-14. [10] Zimbelman J. and Johnson M. (2014) Fall AGU, Abs. EP43B-3564. [11] Howard A. (1977) *Geol. Soc. Am. Bull., 88,* 853-856. [12] Hayward R. et al. (2014) *Icarus*, 230, 38-46.